In: Proceedings of Fourth Conference on Rapid Solidification Technology, eds. R. Mehrabian and M. Cohen, Sta Barbara, Dec. 1986

SHOCK-WAVE CONSOLIDATION OF RAPIDLY SOLIDIFIED METAL POWDERS

MARC A. MEYERS

Center for Explosives Technology Research

Department of Materials and Metallurgical Engineering

New Mexico Institute of Mining and Technology

Socorro, New Mexico 87801

ABSTRACT

Shock consolidation of powders is a one-stage densification/bonding process which presents a potential for rapidly-solidified powders. The shock wave travels through the powder, and inter-particle friction, jetting, and particle deformation cause bonding. Shock consolidation may be carried out by gun (gas gun, electromagnetic gun, powder gun) or explosive techniques. Explosive techniques are most easily implemented and lend themselves to scale-up. However, there are considerable technological difficulties that have not been resolved properly; the principal ones are cracking and net-shape capability.

Recent results obtained on the consolidation of superalloys (Mar M 200, IN 100, IN718), titanium alloys (Ti-6% Al- 4%V, Ti-6% Al- 6%V-2% Sn, Ti-17, and a dispersion-strengthened alloy), and on aluminum-lithium alloys will be discussed. A double-tube technique utilizing explosives was recently developed at the Center for Explosives Technology Research, New Mexico Tech. It yields considerably improved consolidation. Titanium alloy cylinders with 10 kg were successfully consolidated, and scale-up to 100kg seems feasible.

1. INTRODUCTION

Shock consolidation is a powder consolidation method that has been known for over twenty years. Nevertheless, there is no current commercial application of this process, except, perhaps, in the USSR. The production of rapidly solidified powders has revived the interest in this "exotic" consolidation process. The basic mechanism by which consolidation is achieved is (a) deformation of the particles, filling the interstices; (b) friction, impact, and jetting, breaking down surface oxides and creating localized regions of melting. Shock consolidation of metallic powders has recently been reviewed by Gourdin [1]. A number of papers can be found in the proceedings of the 1985 EXPLOMET conference [2], and a NMAB study has been conducted [3].

In this paper, three aspects of shock consolidation will be discussed. First, the techniques used by the author and co-workers will be presented. Second the microstructural and mechanical understanding of shock consolidated rapidly solidified powders gained at the Center for Explosives Technology Research (New Mexico Institute of Mining and Technology) will be reviewed. The following alloys have been consolidated in the 1985-1986 period:

Superalloys:	Mar M-200
	IN 100
	IN 718
Titanium Alloys:	Ti-17
	Ti-6% Al- 6%% V- 2% Sn
	Ti-6% Al- 2% Mo-4% Zr-2% Sn+$Er_2 O_3$
Aluminum Alloys:	Al-Li-Cu (Mg, Zr)
	Al-Fe-Ce

Titanium-aluminum alloys: Ti-Al and Ti_3 Al

Third, the limitations of shock consolidation, the problems with scale-up, and the economics of the process will be briefly discussed.

2. EXPERIMENTAL TECHNIQUES

The shock wave passing through the powder consolidating it can be generated by the following techniques: (a) impact of a projectile against powder; (b) detonation of explosive in direct contact with powder ; (c) deposition of energy at powder or powder-containing surface by other technique, such as pulsed laser. The projectile can be accelerated in a gun (gas, electromagnetic, or (gun) powder) or by means of explosives. Two types of systems have been most commonly used: (a) systems with massive anvils (anvil mass orders of magnitude higher than powder mass); and (b) systems in which the external containment vessels are minimized. Systems with massive anvils have been used for fundamental research in which the stress pulse traveling through the powder was well characterized by computational techniques. They have also been used to consolidate small masses with high value (boron nitride and diamond for cutting tools). The systems developed by Gourdin [2]at LLNL and the excellent calibrated series developed by Graham and co-workers at Sandia National Laboratories [4,5] are the best fundamental research tools. The stress and temperature histories in the capsule containing the powder are well known. The systems used by Sawaoka [6] are designed to produce small, crack-free compacts of ceramics and also require massive tooling. Figure 1(a) shows a section of the Bear series developed by Graham at SNL. Systems in which external tooling is minimized use the balance of the explosive charge to minimize reflections, which can easily produce fracture, since the waves have amplitude greatly exceeding the "spall" strength (dynamic tensile strength) of the powders. The simplest version of this system that has emerged is the cylindrical geometry, shown in Figure 1(b). Detonation starts at the top and produces an "implosion" of the tube, that

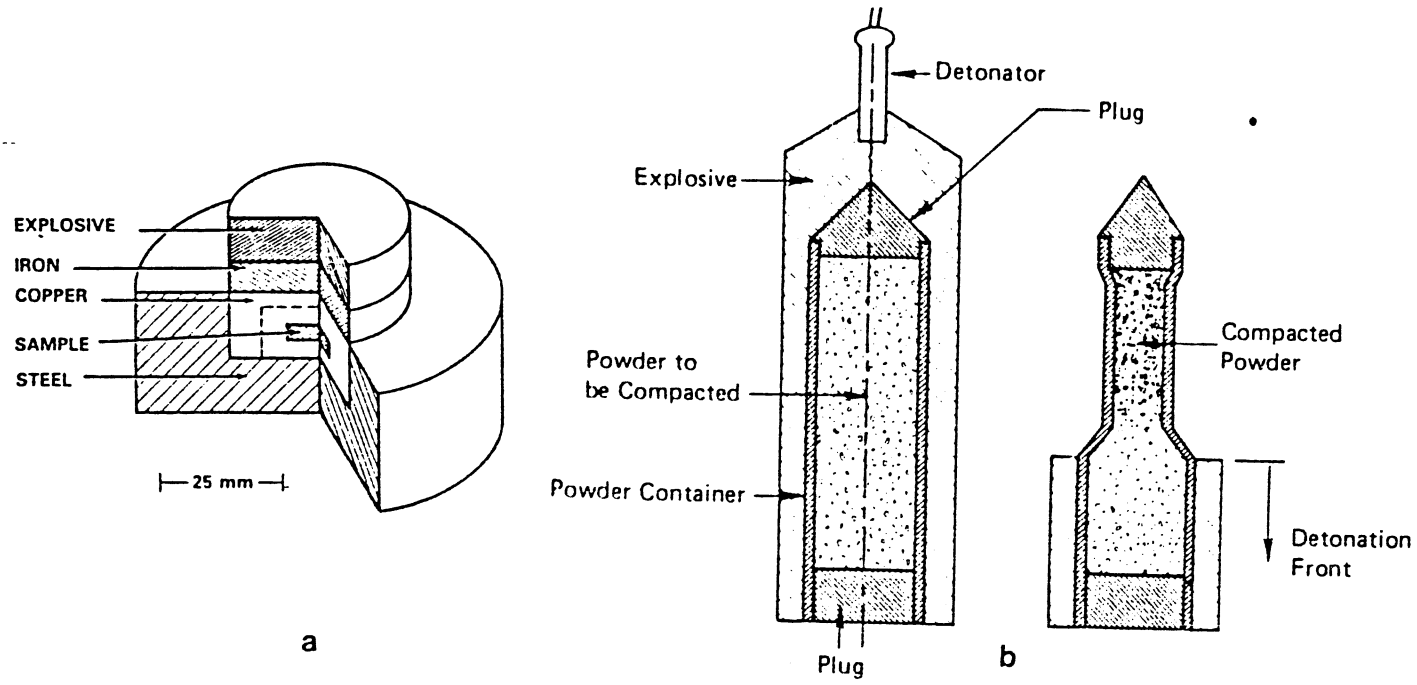

Figure 1 a) Section of calibrated Sandia Bear fixture with capsule containing powder in center.

b) Explosive consolidation in cylindrical geometry; detonation front propagates downward. From [3], p.19.

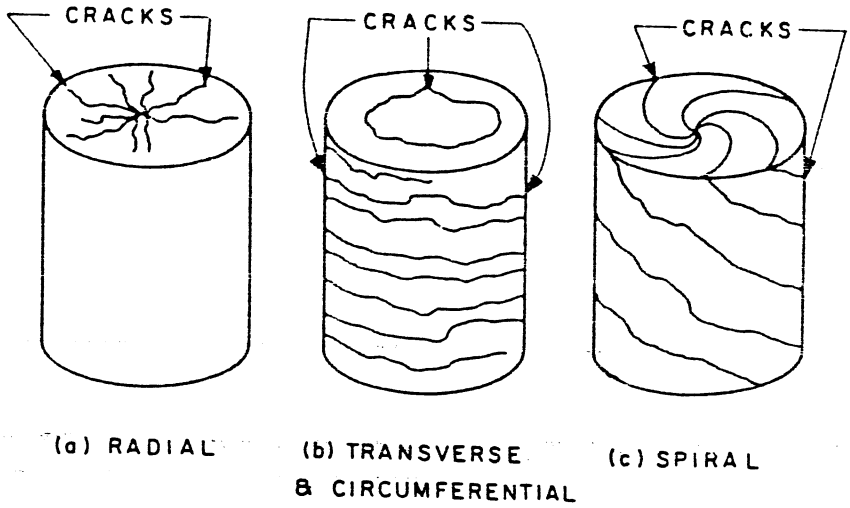

Figure 2 Various types of cracks produced in explosive consolidation using the cylindrical geometry. Adapted from [3], p.88.

contains the powder, as it proceeds downwards. The shock waves in the powder converge from the outside to the inside. This system requires relatively little tooling: a powder container, with top and bottom anvils. The shock waves are axysymetrically balanced and the geometrical convergence is compensated by the attenuation. This system has been used in the majority of the "engineering" studies. The convergent wave pattern and the radially expanding waves create stress patterns that can lead to several modes of cracking, shown in Figure 2. Radial, transverse, circumferential, and spiral (helicoidal) cracks can be observed. An additional problem is a hole often observed along the central axis, produced by a synergistic wave effect at the center generating a Mach stem, with melting.

A modification of the cylindrical fixture shown in Figure 1(b) was developed at the Center for Explosives Technology Research and yields considerably improved consolidates [7]. Figure 3(a) shows the longitudinal section of the system. The essential difference from the system of Figure 1(b) is that an additional tube is placed between the explosive and the metal powder. The external tube (flyer tube) is surrounded by the explosive charge, which is detonated at the top; this external tube acts as a flyer tube impacting the internal tube. This technique generates pressures in the powder that can be several times higher than the ones generated by the single-tube technique. The main advantage of this technique is that it allows the use of low detonation-velocity explosives for consolidating hard powders. The low detonation-velocity explosives minimize cracking in the compacts. The pressure in the powder can be calculated by numerical techniques, or approximated by analytical computations. The velocity of the flyer tube, V_p, can be approximated by

$$V_p = \sqrt{2E}\left[\frac{3}{5\left(\frac{m}{c}\right)+2\left(\frac{m}{c}\right)^2 \frac{R+r_o}{r_o} + \frac{2r_o}{R+r_o}}\right]^{1/2}$$

where E is the Gurney energy, m/c is the ratio between tube and explosive mass, R is the radius of the explosive charge, and r_o is the radius of the flyer tube (Fig. 3 (b)). Equation (1) is a modified form of the Gurney equation [7] developed in the 1940's. It assumes that the chemical energy of the explosive is transformed into kinetic energy of the explosive products and kinetic energy of the flyer plate. The velocity of the detonation products is assumed to vary linearly with distance. Figure 3(c) shows the variation of velocity of the detonation products. At r_o, it is equal to the flyer tube velocity, V_p. At a radius r, it is equal to zero. At the external radius R, it is equal to V_o.

3. MICROSTRUCTURES AND MECHANICAL PROPERTIES

In general, the microstructure of shock-consolidated material is characterized by two distinct regions: (a) the particle interiors, which remain unchanged, upon observation by optical microscopy; however, the deformation substructure observed by transmission electron microscopy is that characteristic of shock hardened materials; (b) the interparticle regions, which exhibit severe plastic deformation and vestiges of interparticle melting and resolidification. Williamson and Berry [8] performed calculations using a two-dimensional hydrocode that predict temperatures in the interparticle regions exceeding significantly the melting point. Figure 4 shows the microstructures of four shock consolidated alloys. Figure 4 (a) shows the superalloy IN 718. The white-etching regions are probably material that is molten during the shock deformation process. This material is then resolidified at a very high rate. The microstructure generated is dictated by the cooling rate during solidification. Figure 4(b) shows a scanning electron micrograph of a Al-Li-Cu-Mg

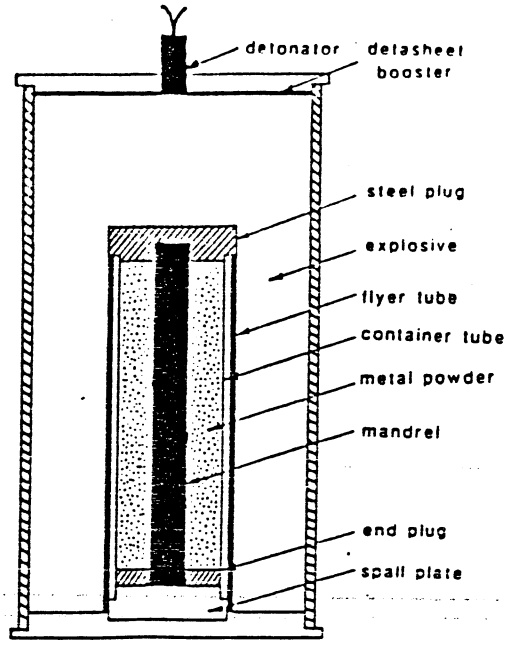

a

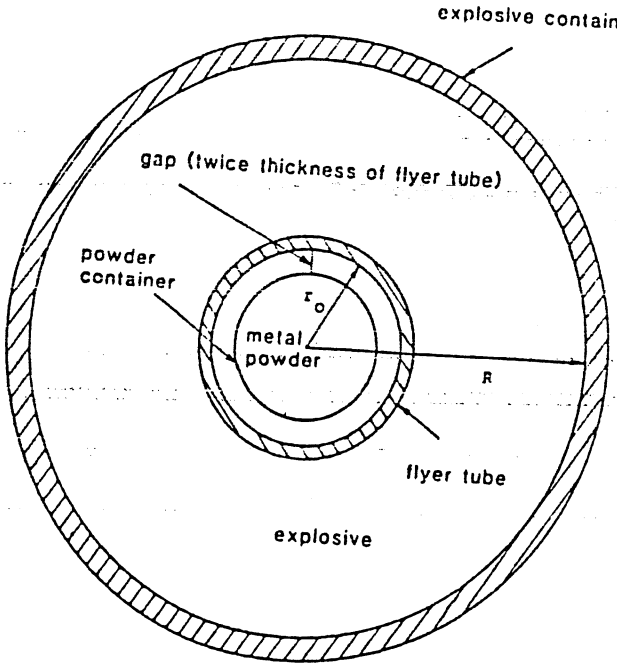

b

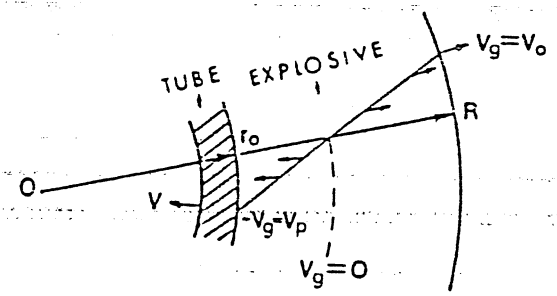

c

Figure 3 (a) Experimental set-up for consolidation using flyer tube technique. Consolidation is initiated at top and propagates downward accelerating flyer tube, that impacts metal powder container; (b) Cross-section of double-tube configuration; (c) Variation of velocity of gas with distance from flyer tube.

a

b

c

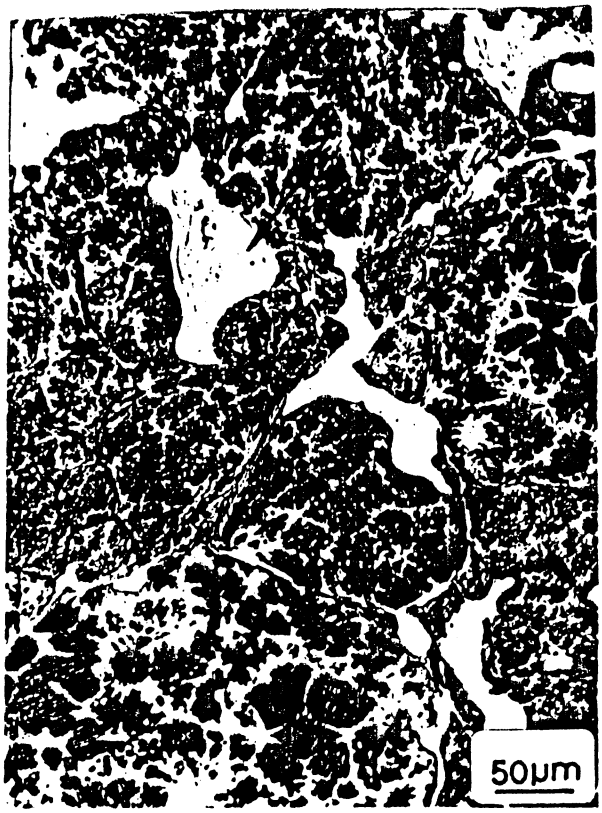

d

Figure 4 Characteristic microstructures of shock consolidated (a) IN718 superalloy; (b) Al-Li alloy (SEM of polished and etched surface); (c) Ti-17 alloy; and (d) Ti_3Al.

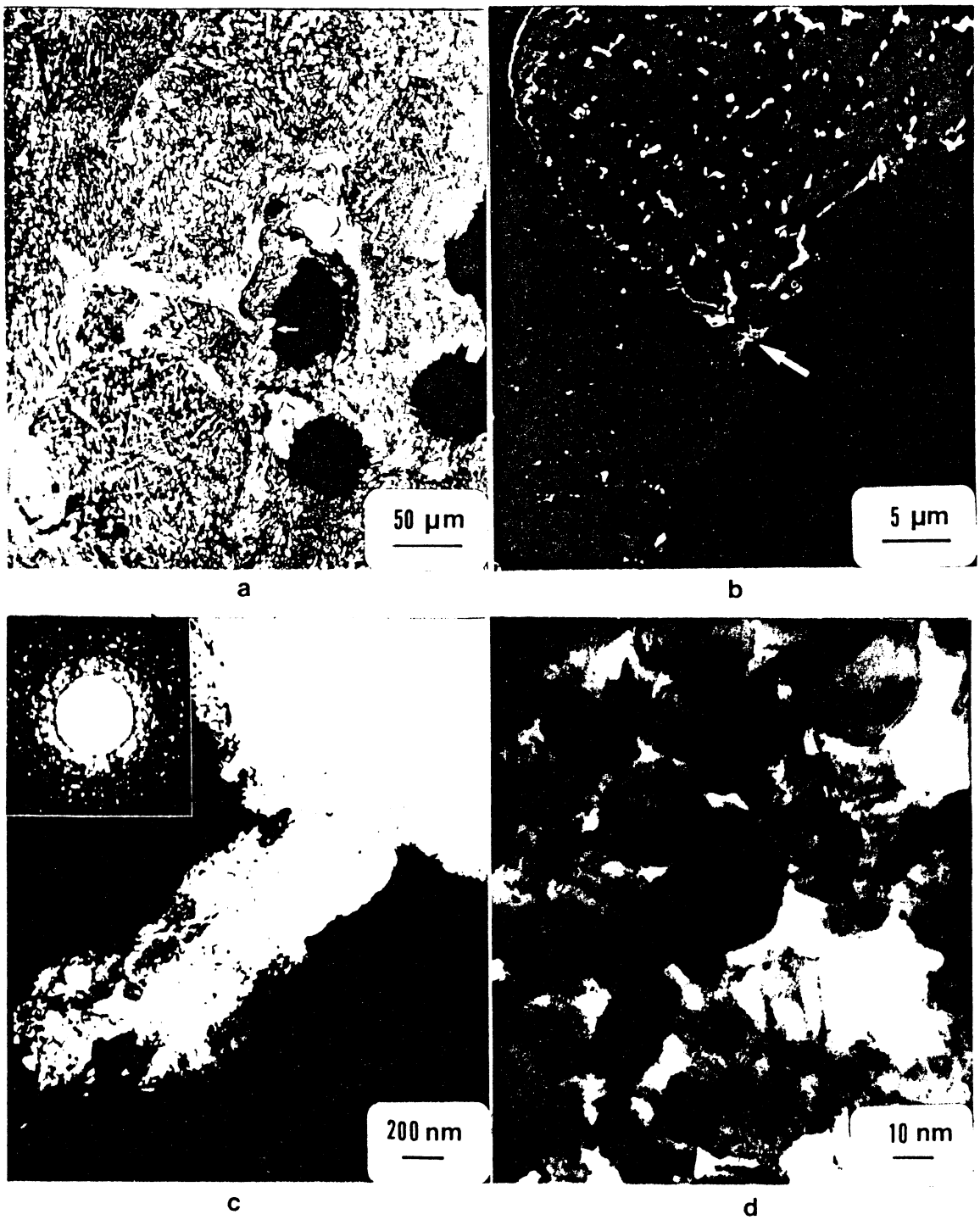

Figure 5 (a) Optical micrograph of hole in IN718 showing (arrow) area observed by transmission electron microscopy; (b-d) Transmission electron micrographs of arrowed area.

alloy. The smooth regions represent the original particles, while the curved "grainy" region is the molten pocket. In Figure 4(c) the titanium alloy Ti-17 is shown. Small molten pockets (shown by arrows) can be seen. These regions do not exhibit the contrast due to microcellular/microdendritc structure. Figure 4(d) shows a titanium aluminide. It is evident that it is well consolidated. The white-etching regions are evidence of melting.

Transmission electron microscopy confirms that the structure of the molten pockets is very different from that of the interior of the powder particles. Figure 5 shows the transmission electron micrograph of a white-etching region in IN 718. Figure 5(a) shows the optical micrograph of the hole with the arrow identifying a small white-etching spot, that is imaged in the transmission electron microscope in Figure 5(d). The grain diameters seem to be of the order of 30nm. The electron diffraction (Fig 5(c)) clearly shows the reflections from numerous individual grains. The absence of dislocations and the microcrystalline structure are evidence of melting and rapid resolidification. Similar results were obtained for titanium alloys, Fig. 6. Figure 6(a) shows the interior of Ti-17 powder consolidated by explosives. A well developed dislocation substructure can be seen. Figure 6(b) shows the interparticle region. It is microcrystalline and free of dislocations. Thus, melting and rapid resolidification probably took place. Figure 6(c) shows a titanium alloy containing erbium after shock consolidation. This powder had a microcrystalline structure. Upon aging the we can see pockets of recrystallized material (free of dislocations). Grain growth is severely inhibited in this alloy, but the erbium oxide dispersion evident in Figure 6(d) is very uniform.

The mechanical properties of shock consolidated alloys are determined, in essence, by the bonding between the particles. If bonding is perfect, the strength of the consolidated material should be equal to the strength of the material that constitutes the particles. However, bonding is only rarely observed to be of even quality. When the energy deposition at the particle surfaces is not sufficient for melting, the material is densified, but frac-

TABLE 1

Tensile Properties of Shock Consolidated Rapidly Solidified Alloys

Material	Y. S. (MPa)	T. S.(MPa)	RA%
* Al-3Li-1Cu-1Mg-0.2Zr		282	
* Al-8.4Fe-7Ce		256	
* Al-3Li-1Cu-0.2Zr		265	
** Ti-17	1,215	1,233	5
** Ti-662	1,118	1,166	2.5
IN 718(RT cons.)	534	761	
IN 718 (cons. at 525 ^{o}C)	877	1,165	
IN 718 (cons. at 740^{o}C)	540	787	
IN 718 (cons at 740^{o}C+ aging)	901	1,239	

* Tests performed by McDonnell Douglas Research Laboratory
** Tests performed by GE

a

b

c

d

Figure 6 Transmission electron micrographs of shock-consolidated titanium alloys (a) Ti-17 - particle interior; (b) Ti-17 - interparticle melting region; (c) Ti-6242 + Er - after consolidation; (d) Ti-6242 + Er - after consolidation and aging.

ture surfaces follow the particle boundary path and the strength of the compact is very low. This is very well explained by the theory proposed by Schwarz et al [9], that predicts quantitatively a "consolidation" window. On the other hand, if substantial interparticle melting takes place, the fracture occurs through the particles. Two contrasting cases are illustrated in Figure 7. In Figure 7(a), the titanium alloy Ti-17 was densified but not consolidated; the particles are deformed, but little bonding is observed. Figure 7(b), on the other hand, shows a typical dimpled morphology of ductile failure. The energy deposited was sufficient for melting and resolidification and the fracture traverses the particles. Thus, one concludes that the strength of shock-consolidated material should approach that of the shock hardened alloy. Table 1 shows the strengths achieved in aluminum, titanium, and nickel-base superalloys. It approximates, and in some case exceeds, that of the monolithic (I/M) material. However, shock consolidation can only rarely be accomplished without flaws. In practice, it is the presence, size, and nature of the flaws (microcracks and microvoids) that limits the strength of shock-consolidated material.

4. LIMITATIONS, SCALE-UP, AND COST

The two main limitations of shock consolidation are cracking and net shape capability. Cracking has been previously discussed [10,11]. Cracking can be produced by tensile reflections, compressive stresses (shear instabilities leading to cracking) or by solidification shrinking. Figure 8(a) shows circumferential and radial cracks in the cross-section of cylindrical aluminum alloy compacts. These cracks can be alleviated and eliminated by design modifications; computer calculations can be very helpful in this matter. Smaller cracks, at the microstructural level, are also often observed. These microcracks can have a very deleterious effect on mechanical properties, especially the low-cycle fatigue, that is one of the most important properties of nickel-base superalloys. RST alloys tend to be high-strength materials in which the load bearing ability is governed by the size of the cracks. Another source of flaws is shown in Fig. 8(b). The white-etching regions are molten and resolidified. Voids are formed in these regions. These voids are produced by solidification shrinkage. These voids can be nucleation sites for cracks.

Net shape capability will probably limit the production to simple shapes, such as cylinders, tubes, and plates. An exception might be small ceramic compacts for cutting tool applications. The unavoidability of flaws in shock consolidated RST alloys will probably require further processing. Thus, shock consolidation should be combined with additional processes, such as HIP, hot extrusion, rolling, or forging. Shock consolidation would be well suited as a component in a multi- stage process. The flaws present after shock consolidation could be healed in subsequent processing.

Scale-up has been attempted at New Mexico Institute of Mining and Technology and does not seem to present problems. Figure 9 shows titanium alloy cylinders of increasing size. The scale in the figure is 12 in. long. The largest cylinder weighs 20 lbs and metallographic observation did not reveal any problems. The method described in Section 2 was used for the calculation of the scale-up parameters. Plans for the production of 200 lb cylinders are underway.

Although it is premature to make an economic feasibility study of the process at the present stage, a few preliminary calculations can be made. As an example, the production of a 200 lb titanium alloy billet (6 in diam; 6.5 ft long) would require 500 lbs of explosive, at a cost of $75 ($0.15/lb). The

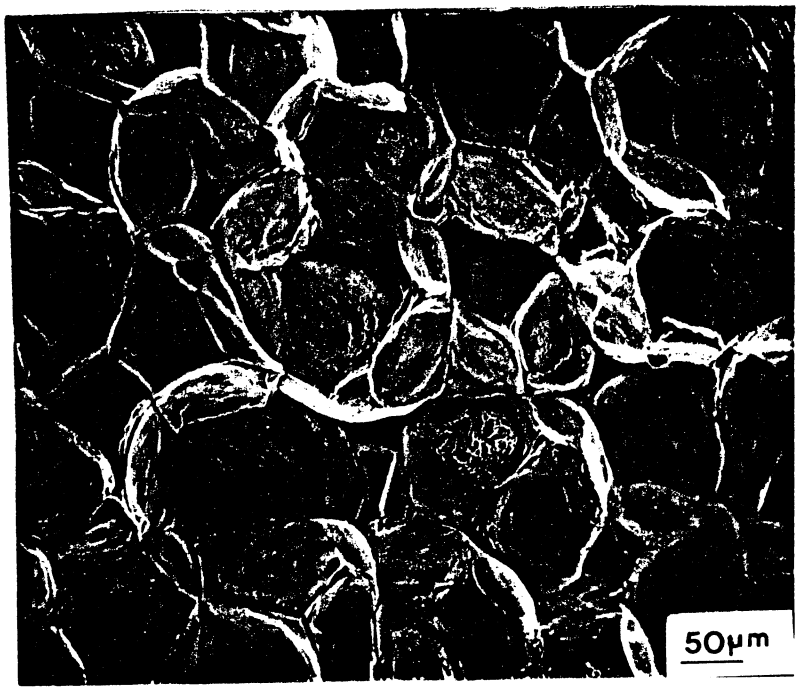

a

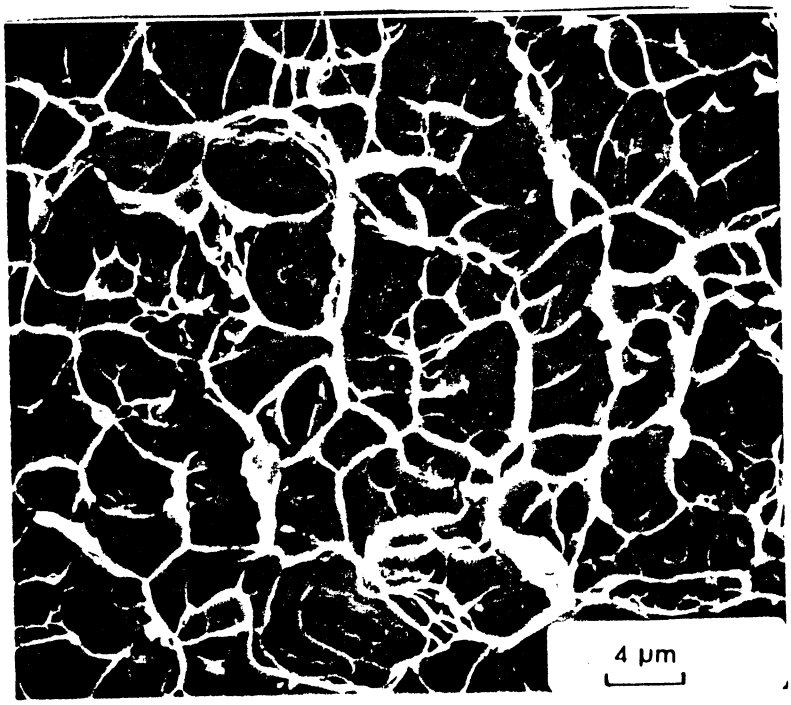

b

Figure 7 Scanning electron micrographs of (a) poorly bonded and (b) well bonded Ti-17 alloy.

tooling costs could be brought down to $300. Field set-up costs per shot could be as low as $200. This would result in a production cost of approximately $3/lb. The daily production of five 200 lb billets (~ 100 tons/year) could be carried out by a small company with a staff of 2-4 persons.

ACKNOWLEDGEMENTS

The research described here was conducted in the period 1981-1986 with support from the National Science Foundation, General Electric, McDonnell Douglas, and the State of New Mexico. Graduate students involved in the work were S. L. Wang, S. N. Yu, H. L. Coker, S. N. Chang, and D. Brasher. Other collaborators were Dr. T. C. Peng (MDRL), Dr. R. Graham (Sandia National Laboratories), Dr. A. Szecket and Dr. N. N. Thadhani (CETR), and Mr. J. Wessells and C. Austin, (GE). The financial support and dedicated work of the collaborators is greatly appreciated. Special gratitude is extended to Mr. Dennis Hunter, of TERA (New Mexico Tech) for overseeing the field experiments, and to Dr. George Mayer (ARO) for inviting me to participate in the Fourth RSP Conference.

a

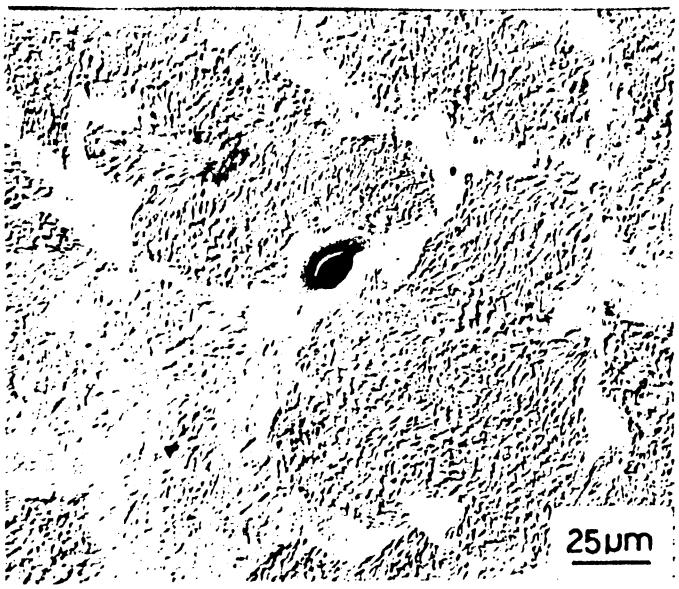

b

Figure 8 (a) Radial and circumferential cracks in cross-section of shock consolidated Al-Li-Cu alloy; (b) Void produced during solidification of molten pool in IN718.

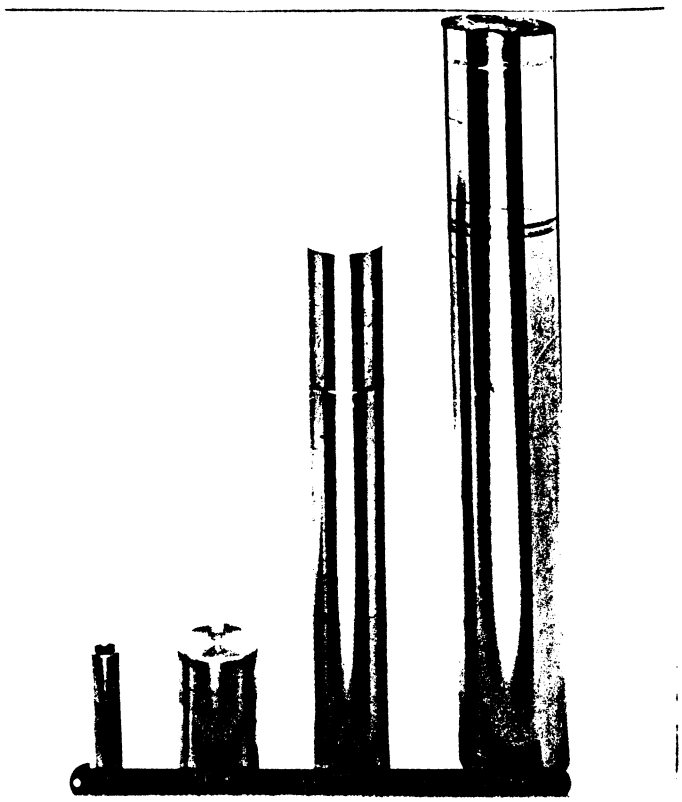

Figure 9 Titanium alloy cylinders shock consolidated (scale 12 in. long).

References

1. W. H. Gourdin, Prog. in Matls. Sci., 30 (1986) 39.

2. L. E. Murr, K.P. Staudhammer and M.A. Meyers, eds., Metallurgical Applications of Shock-Wave and High-Strain-Rate Deformation, M. Dekker, New York, 1986.

3. "Dynamic Compaction of Metal and Ceramic Powders," NMAB-394, National Materials Advisory Board, National Academy of Sciences, Washington, DC, 1983.

4. L. Davison, D.M. Webb, and R.A. Graham in "Shock Waves in Condensed Matter-1981", eds. W.J. Nellis, L. Seaman, and R.A. Graham, American Institute of Physics, 1982, p. 67.

5. R.A. Graham and D.M. Webb, in "Shock Waves in Condensed Matter-1983," eds. J.R. Asay, R.A. Graham, and G.K. Staub, North-Holland, New York, 1984, p. 211.

6. R.A. Graham and A. Sawaoka, High Pressure Explosive Processing of Ceramic, Trans Tech Publications, Switzerland, 1986.

7. M. A. Meyers, S.L. Wang, and A. Szecket, submitted for publication, 1986.

8. R.L. Williamson and R.A. Berry, in "Shock Waves in Condensed Matter - 1985", ed. Y.M. Gupta, Plenum, Press, NY, 1986, p. 341.

9. R.B. Schwarz, P. Kasiraj, T. Vreeland Jr., and T. J. Ahrens, Acta Met., 32 (1984 1243.

10. M.A. Meyers, and H. -r. Pak, J. Mater. Sci., 20 (1985), 2133.

11. S.L. Wang, M.A. Meyers, and R.A. Graham, in "Shock Waves in Condensed Matter - 1985", ed. Y.M. Gupta, Plenum Press, NY, 1986, p. 731.